Generation of Escher Arts with Dual Perception

Shih-Syun Lin, *Member, IEEE*, Charles C. Morace, Chao-Hung Lin, *Member, IEEE*, Li-Fong Hsu, and Tong-Yee Lee, *Senior Member, IEEE*

Abstract—Escher transmutation is a graphic art that smoothly transforms one tile pattern into another tile pattern with dual perception. A classic example is the artwork called Sky and Water, in which a compelling figure-ground arrangement is applied to portray the transmutation of a bird in sky and a fish in water. The shape of a bird is progressively deformed and dissolves into the background while the background gradually reveals the shape of a fish. This paper introduces a system to create a variety of Escher-like transmutations, which includes the algorithms for initializing a tile pattern with dual figure-ground arrangement, for searching for the best matched shape of a user-specified motif from a database, and for transforming the content and shapes of tile patterns using a content-aware warping technique. The proposed system, integrating the graphic techniques of tile initialization, shape matching, and shape warping, allows users to create various Escher-like transmutations with minimal user interaction. Experimental results and conducted user studies demonstrate the feasibility and flexibility of the proposed system in Escher art generation.

Index Terms—Escher art, shape matching, content-aware warping

1 Introduction

The graphic artist Maurits Cornelis Escher (1898-1972) created many attractive artworks with interesting mathematical and human perceptual properties, including symmetry, transmutation, and duality. Duality refers to Escher's arrangement of neighboring shapes that results in a dual perception. Specifically, the figure-ground assignment of neighboring shapes can reverse depending on the viewer's focal attention. Escher intentionally employed dual figure-ground arrangements to reveal the ambiguities of visual perception and categorization. Transmutation, depicted by a gradual shape transition between different tile patterns, serves as a visual device to create temporal and narrative aspects in Escher's artwork. Combining transmutation and duality, Escher emphasized both the individuality and the interdependent relationship of multiple motifs. The unique way of thinking and the artful mathematics of Escher's artworks have thus made a continuous and deep influence in the fields of computer graphics, art, psychology, and commercial design.

Designing a transmutation with dual figure-ground perception has proven to be a difficult task for artists. One challenging aspect is determining compatible shapes that can be aligned so that they share a common boundary. Regarding this difficulty, Escher noted, "*After a great deal of patience and deliberation, and usually a seemingly endless series of failures, a line is finally drawn. It looks so simple that an outsider cannot imagine how difficult it was to obtain*." [1]. Furthermore, using specified shapes to automatically generate a transmutation with dual perception is a difficult problem because it requires that the shapes fit together like pieces of a jigsaw puzzle but still remain recognizable individually. Therefore, the current study aims to provide a system for artists and even general users to generate Escher-like transmutations.

Metamorphosis I to *III* and *Sky and Water I* and *II* are the most famous transmutation artworks created by Escher, which utilize various deformation variations with dual perception. Kaplan [2] classified the deformation variations in Escher's artworks into six types, namely, *realization*, *crossfade*, *abutment (duality)*, *growth*, *sky-and-water*, and *interpolation*. The deformation that transforms a geometric pattern into a landscape or other concrete scene is called realization deformation. In abutment deformation, two motifs having vaguely similar geometric shapes are spliced together along a shared curve. In interpolation and crossfade deformations, a tile pattern evolves into another tile pattern by smoothly deforming the shapes and by fading textures or simplifying feature lines within the tile patterns, respectively. In growth deformation, the shape of a tile is gradually grown to fill or match the figure (or ground) space. The sky-and-water deformation as shown in Fig. 1, integrates the crossfade, abutment, and interpolation deformations to the transition of an object in a space and another object in the dual space. To generate Escher transmutations, we propose a system that integrates several graphic techniques to realize the deformation types of crossfade, abutment, growth, sky-and-water, and interpolation. The proposed system with these deformations has thus the ability to create various Escher-like transmutations for the purposes of visualization, tessellation generation, and efficient commercial design.

- *S.-S. Lin is with the Department of Computer Science and Engineering, National Taiwan Ocean University, Keelung 202, Taiwan, R.O.C. E-mail: linss@mail.ntou.edu.tw.*
- *C.C. Morace, L.-F. Hsu, and T.-Y. Lee are with the Department of Computer Science and Information Engineering, National Cheng Kung University, Tainan 701, Taiwan, R.O.C. E-mail: {charles.c.morace, bee040811}@gmail.com, tonylee@mail.ncku.edu.tw.*
- *C.-H. Lin is with the Department of Geomatics, National Cheng Kung University, Tainan 701, Taiwan, R.O.C. E-mail: linhung@mail.ncku.edu.tw.*

Manuscript received 27 June 2016; revised 8 Dec. 2016; accepted 18 Jan. 2017. Date of publication 27 Jan. 2017; date of current version 29 Dec. 2017. Recommended for acceptance by A. Shamir. For information on obtaining reprints of this article, please send e-mail to: reprints@ieee.org, and reference the Digital Object Identifier below. Digital Object Identifier no. 10.1109/TVCG.2017.2660488

Fig. 1. *Sky and Water I* created by the proposed system.

In this paper, we propose new shape matching, tile arrangement, and shape warping methods to generate Escher-like transmutations with dual figure-ground perception. In shape matching, a curvature signature and shape overlap information are utilized to optimally extract from a database the best-matched shape of a user-specified tile. Users are also allowed to specify two and even several tiles, and the proposed system can automatically generate a transmutation that contains shape transitions of these specified tiles. In addition, a content-aware warping is proposed to generate a shape transition between two tile patterns while preserving their significant feature lines and textures as much as possible. With these methods, the proposed system can generate an interesting and engaging transmutation sequence with dual figure-ground perception using one or several shape transitions, thereby making it desirable for advertising and exhibition.

2 Related Work

Computer-aided generation of graphic arts has become an active research topic in the field of computer graphics because of the practical importance of efficient commercial design. Many methods have been proposed for the automatic generation of various graphic arts, such as image collages [3], ASCII arts [4], shadow arts [5], illusion images [6], micrography [7], and hidden images [8]. Similar to these works that create graphic arts, the aim of our study is to generate Escher-like transmutations by using the techniques of shape matching, tile initialization, and shape warping. However, applying these techniques to the generation of Escher-like artworks is not trivial because of the dual and ambiguous perception in this kind of art. The dual and ambiguous perception comes from the figure-ground arrangement that requires different and deformed tiles to fit together but still remain recognizable individually.

The mathematical structures, smooth shape transitions, and duality property of Escher's artworks have been extensively studied. The related studies have addressed the analysis of mathematical structures in Escher's artworks [9], [10], creating new designs inspired by Escher's artworks [11], and automatically generating Escher-like tessellations [12], [13], [14] or Sky-and-Water transmutations [15]. Kaplan and Salesin [12] introduced a problem, called Escherization, to automatically generate isohedral tiling patterns that are close to a given shape. The tiling covers the plane without gaps or overlaps except at the boundaries of patterns. Kaplan and Salesin [14] also considered dihedral escherization that deals with a tiling generated from two different tile shapes. Adapting their previous tiling generation method, a dihedral tiling is produced by generating an isohedral tiling and then splitting each tile into two differently shaped tiles. To improve the efficiency of the shape escherization, Koizumi and Sugihara [13] reduced this tiling problem to a maximum eigenvalue problem. These tiling methods do not consider textures insides the tiles; thus visually salient features may be undesirably deformed. In our paper, a feature saliency measure is integrated in warping to force the significant features to undergo as-rigid-as-possible deformation.

In addition to the automatic generation of Escher-like tessellations, previous studies have focused on user-friendly interface and tiling techniques for the generation of special Escher-like art. For instance, Yen and Sequin [11] developed an interactive system to design Escher spheres, that is, a set of tiles that are assembled to cover the surface of a three-dimensional sphere. Sugihara [15] proposed a computer-aided system that allows users to create Escher-like Sky-and-Water transmutations. By contrast, the proposed system in this paper focuses on the dual and ambiguous perception and the deformation variations, including cross-fade, abutment, growth, sky-and-water, and interpolation, in Escher's artworks; thus, various Escher-like transmutations can be generated.

Dual figure-ground perception is a distinguishing characteristic in Escher's tiling and transmutation artworks, and many studies have addressed this special perception in relation to Gestalt psychology [16], [17], [18], [19]. These studies discussed the factors that contribute to figure-ground organization. They concluded that the main factors influencing figure and ground assignments are past experience, attention, and intentions, as well as several geometric factors, including convexity, similarity, and color homogeneity. In addition, Schattschneider [20] and Kaplan [2] studied the figure-ground aspect and deformation variation aspect, respectively, of Escher art. In this study, several graphic techniques based on concepts and aspects from these two papers are proposed to generate Escher arts with dual perception. In summary, compared with the related works on the generation of Escher-like artworks [12], [15], our paper provides the contribution of implementing the main deformations and figure-ground arrangements used in Escher's artworks, thereby a variety of Escher-like transmutations can be generated with minimal user interaction or even automatically.

3 Methodology

3.1 System Overview

Fig. 2 schematically illustrates the workflow of the proposed system, which consists of three major steps, namely, *tile initialization*, *shape matching* and *content-aware shape transmutation*. The input to the proposed system is the number of shape transitions and a user-specified tile, which is viewed as the source tile of the transmutation. In tile initialization, a contour with proper convexity is determined for figure-

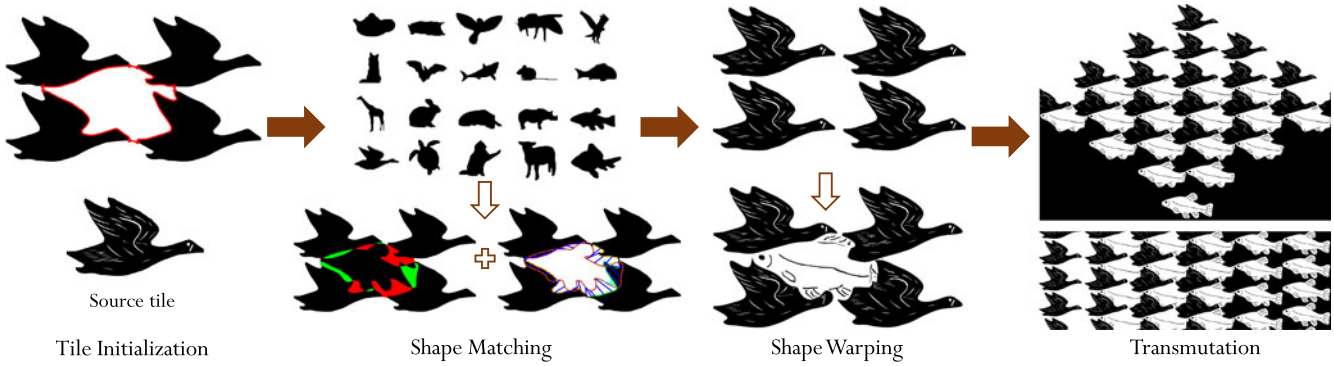

Fig. 2. Workflow of the proposed system. From left to right: Tile initialization, shape matching, shape warping, and transmutation generation.

ground arrangement by the surrounding source tiles. The determined contour is used as a query to search for a tile with the best-matched contour from a database using a two-phase shape matching method. In the first phase, the method based on curvature signature [21] is adopted to align the determined contour and each tile in the database, and to obtain the contour correspondence. In the second phase, a region-based shape similarity is proposed to extract the best-matched tile from the database. With the aid of shape correspondence, in the next step, a content-aware shape transmutation is proposed to generate a smooth shape transformation of the input and retrieved tiles while preserving feature lines inside the tiles as much as possible.

3.2 Tile Initialization

The current study addresses the generation of a two-tile Escher transmutation with dual figure-ground perception. To begin, a tile is arranged in the figure space, and another tile is located in its dual space, that is, the ground space. The input to the proposed method is a user-specified tile, called the source tile, which is initially the figure. In the step of tile initialization, the contour of a tile with a boundary defined by the surrounding four source tiles, called the virtual tile as shown in Fig. 3, is extracted for the determination of the ground tile. In the first step, the contour of the source tile T^S, denoted by $\mathrm{C}(T^S) = \{c_k^S\}_{k=1}^{n_b}$ (where n_b represents the number of boundary points), is extracted using a connected component extraction method. Given four contours of the source tiles $\mathrm{C}(T_a^S)$, $\mathrm{C}(T_b^S)$, $\mathrm{C}(T_c^S)$, and $\mathrm{C}(T_d^S)$ which are arranged in a regular grid pattern in the figure space, the step of tile initialization is to determine the contour of a virtual tile T^V in the ground space, which is denoted as $\mathrm{C}(T^V) = \{c_a^V \in \mathrm{C}(T_a^S), c_b^V \in \mathrm{C}(T_b^S), c_c^V \in \mathrm{C}(T_c^S)$, and $c_d^V \in \mathrm{C}(T_d^S)\}$. To maintain the tile shape and to make the shape

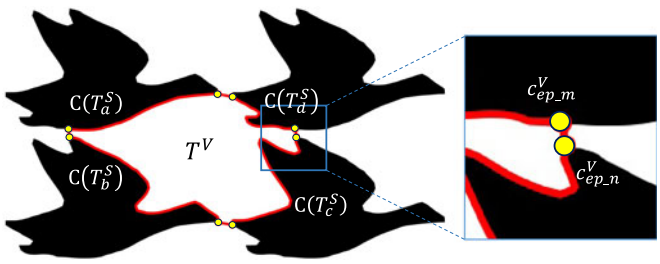

Fig. 3. Illustration of tile initialization. The virtual tile T^V is surrounded by the source tiles T_a^S, T_b^S, T_c^S, and T_d^S.

recognizable, the tiles are positioned in a grid with a 10-pixel buffer. To obtain a virtual tile with a detailed boundary contour, two terms, namely, *closeness*, and *curvature*, are introduced in the objective function. The curvature term is defined according to the curvatures of points on the boundary contour of the virtual tile, that is, $E_{cur}(\mathrm{C}(T^V)) = \sum_{i=1}^{n_v} \frac{1}{Cur(c_i^V)}$, where $Cur(c_i^V)$ represents the discrete curvature of the contour point c_i^V and the curvature is calculated by using the contour of the source tile. A high-curvature contour is preferred because high-curvature curves generally correspond to significant shape information. The closeness term is defined as the distance between the end points in the contour of the virtual tile, that is, $E_{clo}(\mathrm{C}(T^V)) = \sum \|c_{ep\_m}^V - c_{ep\_n}^V\|$, where $c_{ep\_m}^V$ and $c_{ep\_n}^V$ represent the end points of a sub-contour and its neighboring sub-contour. With this definition, the space between the initial tiles can be reduced as much as possible. By combining these two terms, the objective function is formulated as

$$E(\mathrm{C}(T^V)) = Nor(E_{cur}(\mathrm{C}(T^V))) + Nor(E_{clo}(\mathrm{C}(T^V))), \quad (1)$$

where $Nor(\cdot)$ is the function to normalize the input quantities into the range $[0, 1]$. The optimal solution is obtained by exhaustively searching among all possible candidates.

3.3 Shape Matching

A two-phase shape matching method is proposed to search a database for the tile that best matches the shape of the virtual tile. This best-matched tile is called the target tile. In the first phase, the planar curve matching method [21] is adopted to align the virtual tile with a tile in the database, and also to obtain their contour correspondence. This curve matching method is based on the integral of unsigned curvatures which is invariant under similarity transformation. Therefore, we can obtain the contour correspondence and similarity transformation, including rotation, scaling, and translation, between two tiles by using this shape descriptor. In the second phase, a new shape similarity metric is proposed to retrieve the tiles similar to the virtual tile in shape, from the database. This similarity metric consists of two factors, namely, *shape similarity*, and *shape consistency*. Given a source tile T^S, a virtual tile T^V, and a curve-matched target tile T^T, the regions occupied by these three tiles are denoted as $R(T^S)$, $R(T^V)$, and $R(T^T)$, respectively. The factor of shape similarity is defined based on overlapping regions, that is,

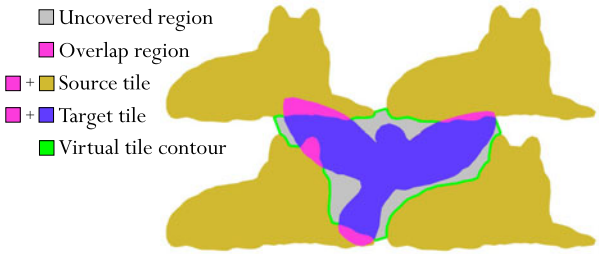

Fig. 4. Illustration of the region-based shape similarity metric. The gray and pink regions represent the uncovered and overlap regions, respectively.

$$F_{sm} = (Area(R(T^V) \setminus (R(T^V) \cap R(T^T))) + Area(R(T^S) \cap R(T^T)))/max_R, \quad (2)$$

where $Area(R(T^V) \setminus (R(T^V) \cap R(T^T)))$ represents the uncovered regions of the virtual tile (the gray region), and $Area(R(T^S) \cap R(T^T))$ denotes the overlap regions of the source and target tiles (the pink region), as shown in Fig. 4. The maximum area max_R is used to normalize F_{sm} to the range $[0, 1]$. In the ideal case, the region of the target tile $R(T^T)$ is equal to that of the virtual tile $R(T^V)$. In addition, the target and source tiles share the same boundaries, meaning that these two tiles are partially matched without gaps.

The factor of shape consistency is used to measure the quality of the obtained contour correspondence. Given a correspondence between the contours of the virtual and target tiles, denoted by $CP^T = \{(p_i^V, p_i^T) | p_i^V \in \mathrm{C}(T^V), p_i^T \in \mathrm{C}(T^T)\}_{i=1}^{n_c}$ (where n_c represents the number of corresponding pairs of points), the shape consistency F_{sc} is defined as the number of intersections in the line segments connecting the corresponding points (the brown lines in Fig. 6 right) and the standard deviation of the displacements between the corresponding points, that is,

$$F_{sc} = \frac{\sqrt{\frac{1}{n_c}\sum_{i=1}^{n}(x_i - \bar{x})^2}}{max_A} + \frac{Insec(CP^T)}{max_B}, \quad (3)$$

where $x_i = p_i^T - p_i^V$ and $\bar{x} = \frac{1}{n_c}\sum_{i=1}^{n_c} x_i$; The function $Insec(CP^T)$ returns the number of intersections in the contour correspondence CP^T; and max_A and max_B are the maximum values used to normalize the quantities into the range $[0, 0.5]$. By combining these two factors, the similarity metric for the tile T^T with the corresponding pair set CP^T is formulated as

$$SSim(T^T, CP^T) = F_{sm}(T^T) + F_{sc}(CP^T). \quad (4)$$

By utilizing the similarity metric in Eq. (4), several tiles in the database can be retrieved. Our system can provide several top-ranked tiles for users to choose from or automatically retrieve the first ranking tile as the target tile.

3.4 Content-Aware Shape Transmutation

The proposed shape transmutation comprises two main steps, namely, *significance measurement* and *content-aware shape warping*, in which the source and target tiles are deformed to fit together while preserving the significant content of tiles. These two steps are described in the following sections.

3.4.1 Significance Measurement

To generate a dual figure-ground arrangement and to increase the recognizability of the deformed tiles, each feature line inside the tile is assigned a value to represent its contribution to the tile's recognition. The tile's boundary contour and feature lines are extracted respectively using connected component extraction techniques. The significance value of a feature line is defined according to its length, sparsity, and regularity. The length of a feature line f_i is defined as the number of pixels in f_i normalized by the maximum length.

$$Len(f_i) = \frac{length(f_i)}{max_{i\in[1,\ldots,N]}\{length(f_i)\}}. \quad (5)$$

To simplify the calculation of feature line sparsity, each line is represented by its centroid, and the sparsity is defined as measuring the distances between the centroids of feature lines, that is, $sparsity(f_i) = \sum_{j=1, j\neq i}^{N} \|\mu_i - \mu_j\|$. By normalizing with the maximal sparsity, the equation is formulated as,

$$Spa(f_i) = \frac{sparsity(f_i)}{max_{i\in[1,\ldots,N]}\{sparsity(f_i)\}}. \quad (6)$$

The shape regularity is computed using the standard deviation of the contour points of a feature line. The contour of f_i is represented by sample points $O_i = \{x_1, \ldots, x_{n_o}\}$, where n_o denotes the number of sample points. The standard deviation of the distances between the sample points and their mean is obtained by $l_{i_\sigma} = \sqrt{\frac{1}{n_o}\sum_{x\in O_i}(x - \mu_i)^2}$. By normalizing with the maximal value, the shape regularity is defined as,

$$Reg(f_i) = 1 - \frac{l_{i_\sigma}}{max_{i\in[1,\ldots,N]}\{l_{i_\sigma}\}}. \quad (7)$$

Note that if l_{i_σ} is small, the $Reg(f_i)$ is large, e.g., a circle or a square would have higher value of $Reg(f_i)$.

By combining the factors of length, sparsity, and regularity, the significance value of a feature line is formulated as,

$$Sig(f_i) = \frac{1}{3}(Len(f_i) + Spa(f_i) + Reg(f_i)). \quad (8)$$

With the Eq. (8), a high significance value is assigned to a long feature line with regular shape, such as a circle, based on the fact that people can more easily perceive deformation of regular shapes than deformation of irregular shapes. Moreover, a high significance value is assigned to a feature line lying in a high-sparsity region, i.e., a region containing few feature lines, based on the fact that the removal of this kind of line will reduce the tile recognition significantly.

Assigning a significance value to each feature line enables the proposed system to generate a crossfade deformation, i.e., gradually reducing content complexity during the shape transition. This idea is inspired by Escher artworks such as *Sky and Water I* and *II*. An example of feature line simplification is shown in Fig. 5. The feature lines are

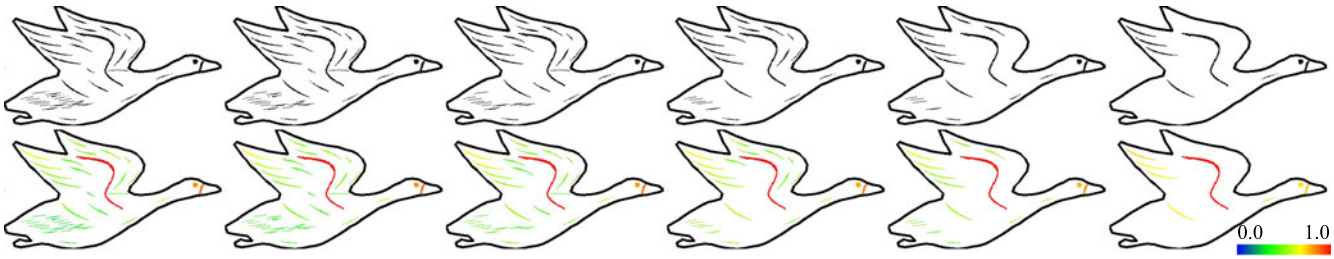

Fig. 5. Example of feature line simplification. Top: Progressive feature line simplification; bottom: Significance values of feature lines ranging from blue (the lowest significance) to red (the highest significance).

progressively simplified based on their significance values. The simplified features represent the tile's interior characteristics well because of the appropriate significance measurement.

3.4.2 Content-Aware Warping

A triangle mesh $\mathbf{M} = (\mathbf{M^S}, \mathbf{M^T})$ that contains two submeshes covering the source and target tiles is created by using Delaunay triangulation [22]. The internal points are generated by that algorithm to maintain the Delaunay property of the triangulation. The submeshes containing a vertex set $\mathbf{V} = \{v_1, \ldots, v_{n_v}\}$, an edge set $\mathbf{E} = \{e_1, \ldots, e_{n_e}\}$, and a triangle face set $\mathbf{F} = \{f_1, \ldots, f_{n_f}\}$ are used as control meshes to drive the tile warping. In addition, a contour correspondence, denoted as $\mathbf{G} = \{(v^S_{m(i)}, v^T_{n(i)}) | v^S_{m(i)} \in \mathbf{M^S}, v^T_{n(i)} \in \mathbf{M^T}\}_{i=1}^{n_g}$, between the boundary vertices of the source and target tiles is established through the correspondence CP^T obtained in shape matching. $m(\cdot)$ and $n(\cdot)$ in $\mathbf{G}$ are the index mapping functions that map the variable i to the vertex indices of the source and target submeshes, respectively. By integrating the significance values of feature lines with the control mesh, each triangle face is assigned a significance value. The face significance is defined as the average significance values of the feature lines inside that triangle face, and then the obtained face importance values are normalized into the range $[0.1, 1]$. The goals are to deform the source tile in the figure space to fit the target tile in the dual space and to generate a smooth shape transition between these two tiles while preserving the shapes and feature lines. To achieve these goals, three constraints, namely, *shape preservation*, *control point*, and *smoothness*, are applied to the control mesh with an optimization solver. These three constraints are described as follows.

Shape Preservation Constraint. To preserve the significant feature lines, this constraint is defined to force the high-significance faces of the control mesh to undergo similarity transformation during warping. Thus, this constraint is formulated as measuring the rigidity of faces

$$\Psi_{sp} = \sum_{i=1}^{n_f} w_i \times \sum_{f_i=(e_{i1},e_{i2},e_{i3})} (\|e'_{i2} - \mathbf{T}^i_{12} e'_{i1}\|^2 + \|e'_{i3} - \mathbf{T}^i_{13} e'_{i1}\|^2), \tag{9}$$

where w_i is the triangle significance value, and e'_i represents the deformed edge of the face f_i. T^i_{12}, containing a scale factor and a rotation factor, is the geometric transformation between e_{i1} and e_{i2}, and T^i_{13} is the geometric transformation between e_{i1} and e_{i3}. Therefore, this constraint measures the changes of the geometric relations of the edges belonging to a face during warping. In other words, a high-significance face is forced to be more rigid during warping.

Control Point Constraint. The control point constraint is defined to force the boundary contour of the source tile to match the contour of the target tile. Thus, this constraint is formulated as measuring the distance between the deformed corresponding boundary vertices $v^S_{m(i)}$ and $v^T_{n(i)}$

$$\Psi_{cp} = \sum_{(v^S_{m(i)}, v^T_{n(i)}) \in \mathbf{G}} \|v'^S_{m(i)} - v^T_{n(i)}\|^2. \tag{10}$$

Smooth Boundary Constraint. To avoid an unsmooth boundary, a smooth constraint is introduced in the optimization for the boundary contours. The first difference method is applied to the boundary vertices, that is,

$$\Psi_{sb} = \sum_{v^S_{m(i)} \in \mathbf{M^S}} \|2 \times v'^S_{m(i)} - v'^S_{m(i-1)} - v'^S_{m(i+1)}\|^2. \tag{11}$$

Warping Optimization. By combining these three constraints, the optimization is formulated as

$$\arg\min_{\mathbf{V'}} \ (\alpha \times \Psi_{sp} + \beta \times \Psi_{cp} + \gamma \times \Psi_{sb}), \tag{12}$$

$$\text{subject to: } \begin{cases} v'_{i1_x} - v'_{i2_x} >= \varepsilon, & \text{if } v_{i1_x} > v_{i2_x} \\ v'_{i2_x} - v'_{i1_x} >= \varepsilon, & \text{if } v_{i1_x} < v_{i2_x} \\ v'_{i1_y} - v'_{i2_y} >= \varepsilon, & \text{if } v_{i1_y} > v_{i2_y} \\ v'_{i2_y} - v'_{i1_y} >= \varepsilon, & \text{if } v_{i1_y} < v_{i2_y}, \end{cases} \tag{13}$$

where α, β, and γ are the coefficients for balancing the contributions of the constraints Ψ_{sp}, Ψ_{cp}, and Ψ_{sb}, respectively. The coefficients α and γ are set to $\frac{1-\beta}{2}$, and β is assigned according to the transmutation progression ranging from 0 to 1. $\mathbf{V'} = \{v'_1, \ldots, v'_{n_v}\}$ is the optimal solution. To avoid the occurrence of mesh foldover, the hard constraints in Eq. (13), which check the consistency of the face normals,

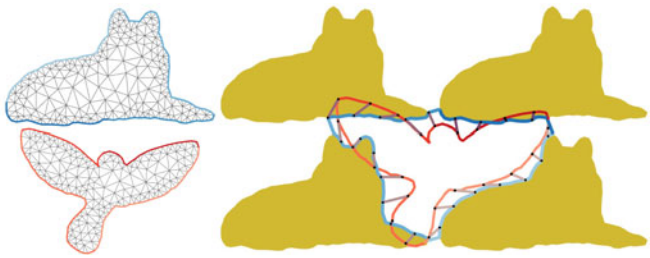

Fig. 6. Illustration of the control mesh (left) and contour correspondence (right). The control mesh covers the source and target tiles, and the correspondence defines the mapping between the boundary contours of these two tiles.

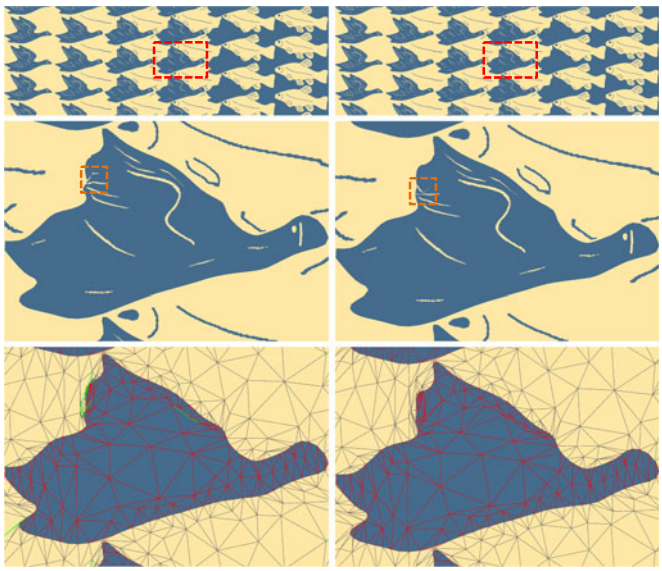

Fig. 7. Comparison between warping with (right) and without (left) foldover-free constraints. The subfigures in the middle are the close-up views of the warping results shown in the top. The deformed meshes are shown in the bottom. The flipped triangles are marked by green. The foldover-free result (right) is obtained using the warping with foldover free constrains.

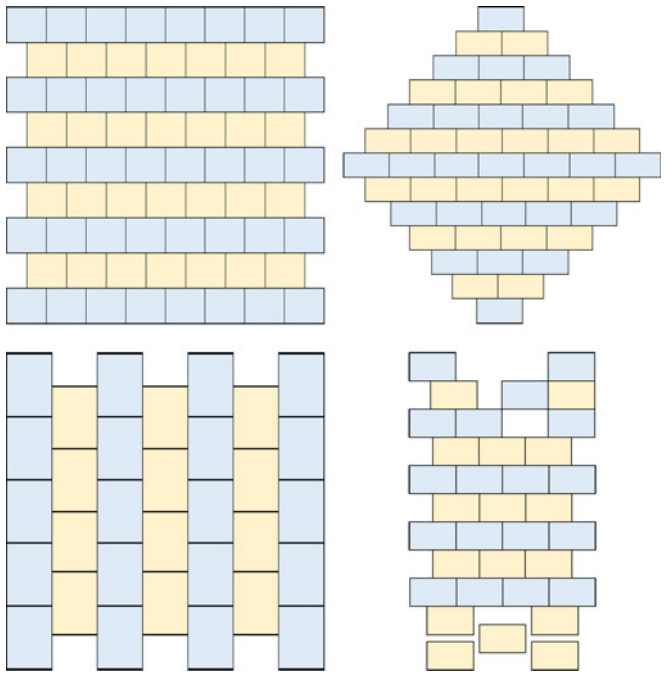

Fig. 8. Tile templates. Top: Vertical tile pattern and sky-and-water tile pattern; bottom: Horizontal tile pattern and less regular tile pattern.

are added in the optimization, where $\varepsilon = 0.001$ is the minimal tolerance scalar of the edge; v_{i1}, v_{i2} represent the vertices of the original edge e_i, and v'_{i1}, v'_{i2} represent the vertices of the edge e'_i in the deformed mesh. An example of the foldover-free mesh deformation is shown in Fig. 7. The foldover problem is solved by using the foldover-free constraints in Eq. (13). In this optimization, a constrained linear least-squares system with a sparse design matrix is obtained from Eq. (12). This constrained linear system is solved using the interior point method [23]. The iterative process of the interior point method is terminated when the movements of the vertices are smaller than a specified threshold value.

3.4.3 *Tile Template Selection and Transmutation*

This study addresses the shape matching and warping of tiles rather than automatic tile tessellation. Therefore, four templates, vertical, horizontal, less regular and sky-and-water tile templates shown in Fig. 8 are created manually in accordance with Escher's artworks, and these tile templates are provided in the proposed system. The users can select a tile arrangement from these templates. In addition, the source and target tiles are assigned two colors with high contrast to create a clear dual figure-ground perception.

In the generation of Escher transmutations, the shape transformation of the source and target tiles is combined with the feature line simplifications. In the figure space, the shape of the source tile is progressively deformed to fit that of the target tile while the feature lines are gradually reduced according to their significance values, creating the effect of dissolving the source tile into the background. In addition, a uniform number of feature lines are removed in each simplification step. Simultaneously, the shape and feature lines of the target tile in the ground space gradually emerge from the background. If a transmutation with more than two types of tiles is required, the target tile is turned into the source tile, and this new source tile is used to retrieve the next target tile from the database after each transmutation. Our system also allows users to specify the tiles in the transmutation. With the aids of shape matching, tile transformation, progressive feature line simplification, and the tile templates, an Escher-like transmutation can be generated even when the input tiles have significant differences in shape.

4 Experimental Results

4.1 Tiling and Deformation Variations

Combining the shape matching, content-aware transmutation, and tile templates with dual figure-ground arrangement enables the proposed system to generate various

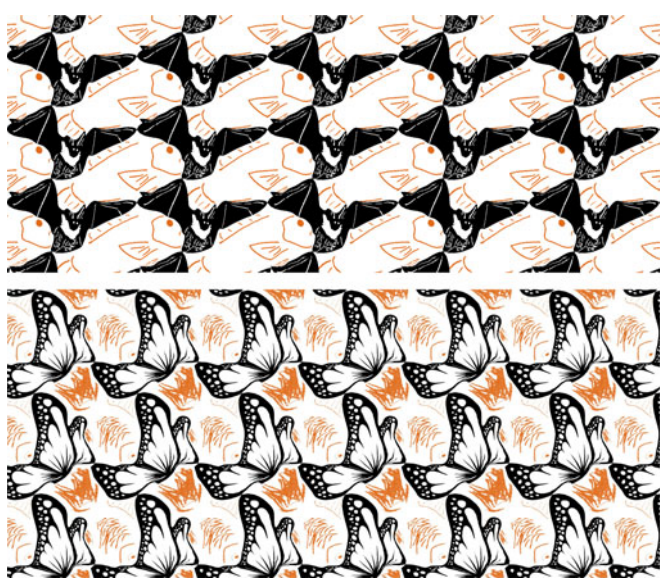

Fig. 9. Two-tile tessellation results. Top: Bat and fish tiles; bottom: Butterfly and fish tiles.

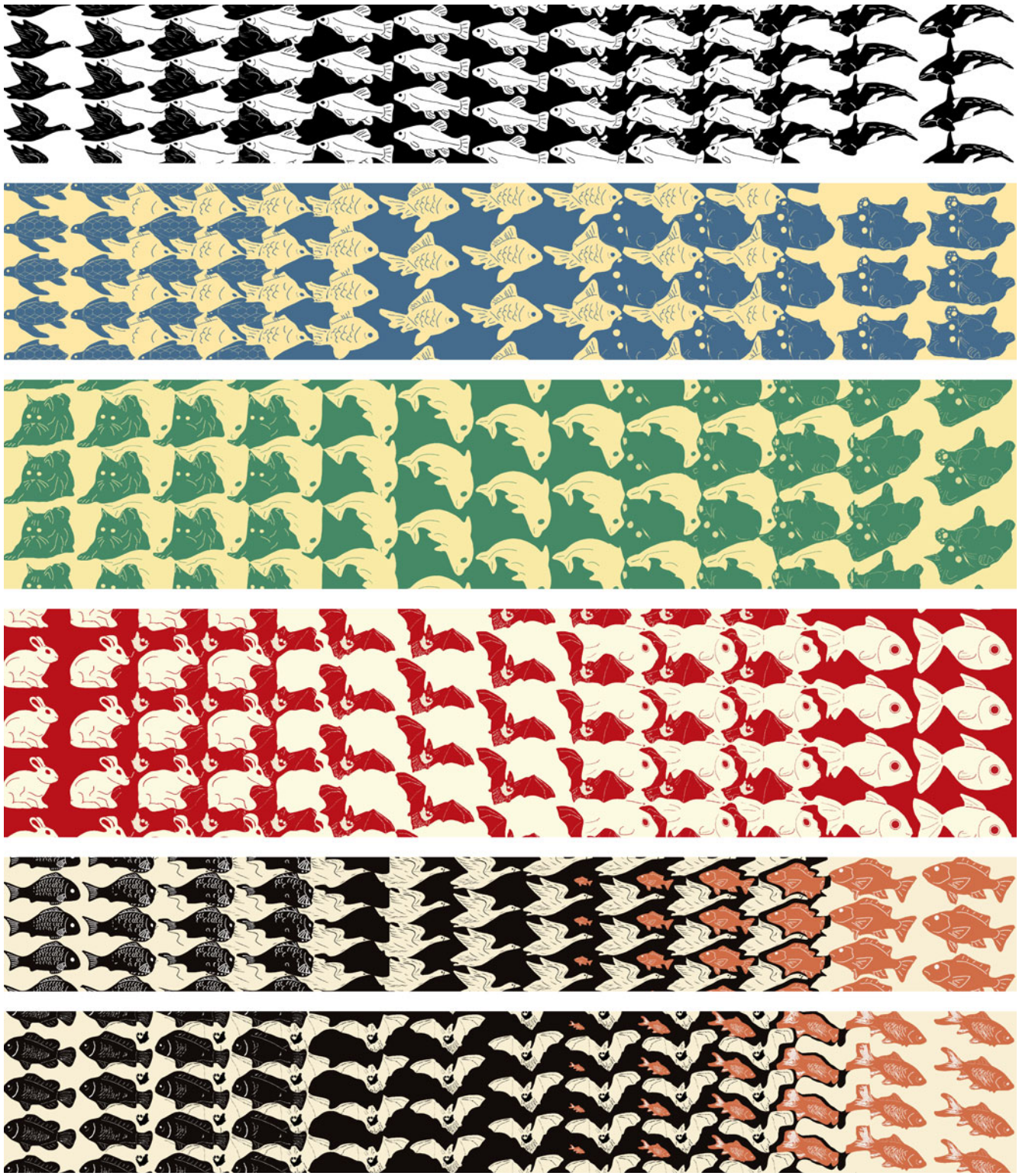

Fig. 10. Generated Escher-like transmutations. The tiles appearing in the beginning of the transmutations are selected by users, and the other tiles are determined automatically using the proposed shape matching.

deformations and tilings used in Escher's arts. First and foremost, a two-tile tiling can be generated. The input two tiles are assigned different colors and the tiles are deformed to fit the shapes together without any gap while the deformed tiles still remain recognizable. Examples of two-tile tilings are shown in Fig. 9. Our system allows users to select the source and target tiles. The selected tiles are deformed to fit together while the feature lines inside the tiles are preserved as much as possible. In this case (Fig. 9), the weight β of objective function (Eq. (12)) is set to 0.5. Second, the proposed shape interpolation and the provided tile templates enable our system to produce a smooth transmutation with dual figure-ground perception. As shown in Fig. 10 (1^{st} row), the transformation sequence between the fish and swan tiles is generated, and these two tiles are arranged in a dual figure-ground arrangement, that is, the

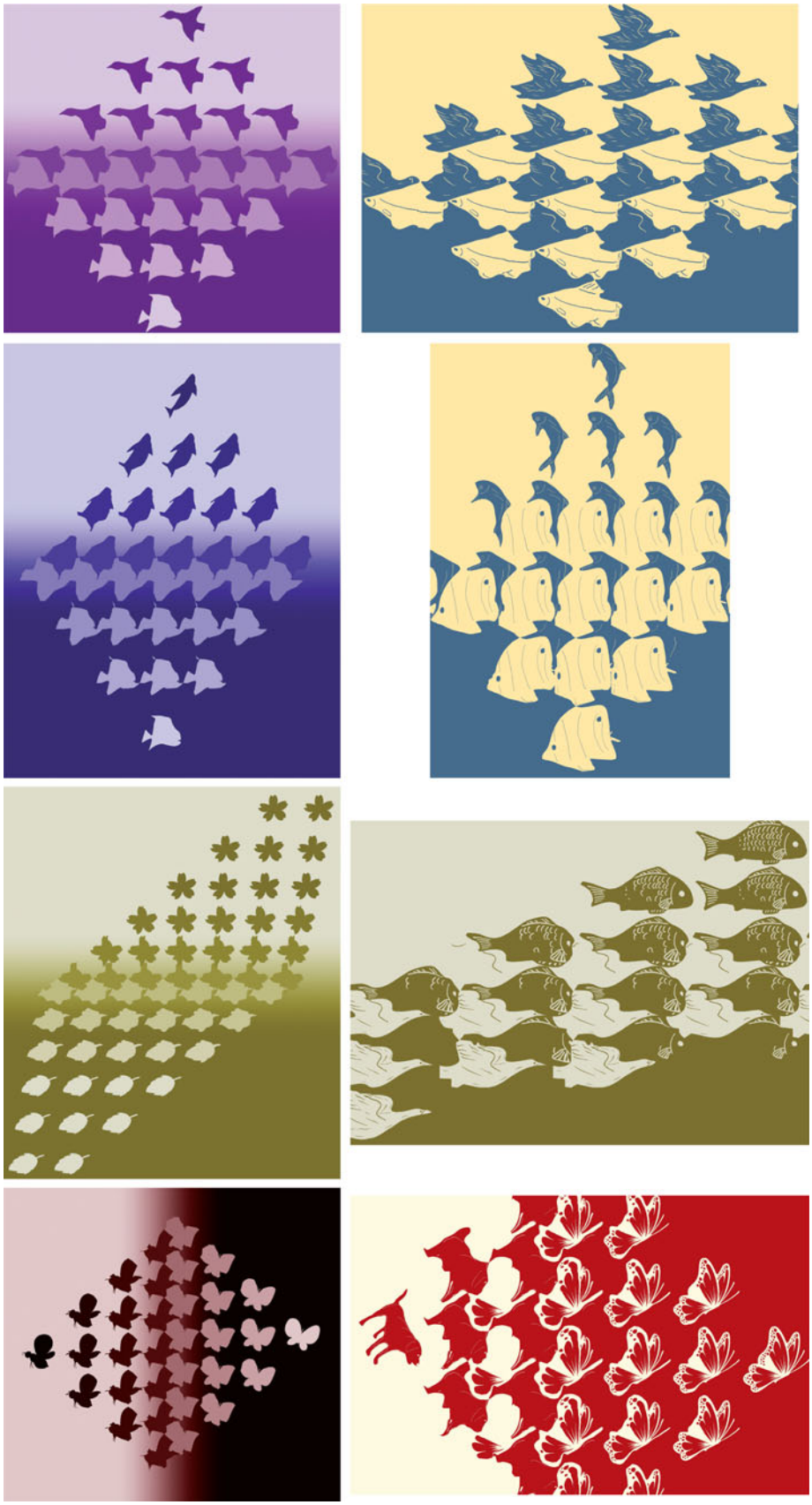

Fig. 11. Comparison between the results of [15] (left) and our results (right).

fish and swan tiles are spliced together along a shared curve. Third, the growth deformation used in Escher's artworks is realized in the proposed scheme with a scaling operation. Two examples of the transmutation using growth deformation are shown in Fig. 10 (5^{th} and 6^{th} rows). A fish tile grows during the shape transition until this tile is well

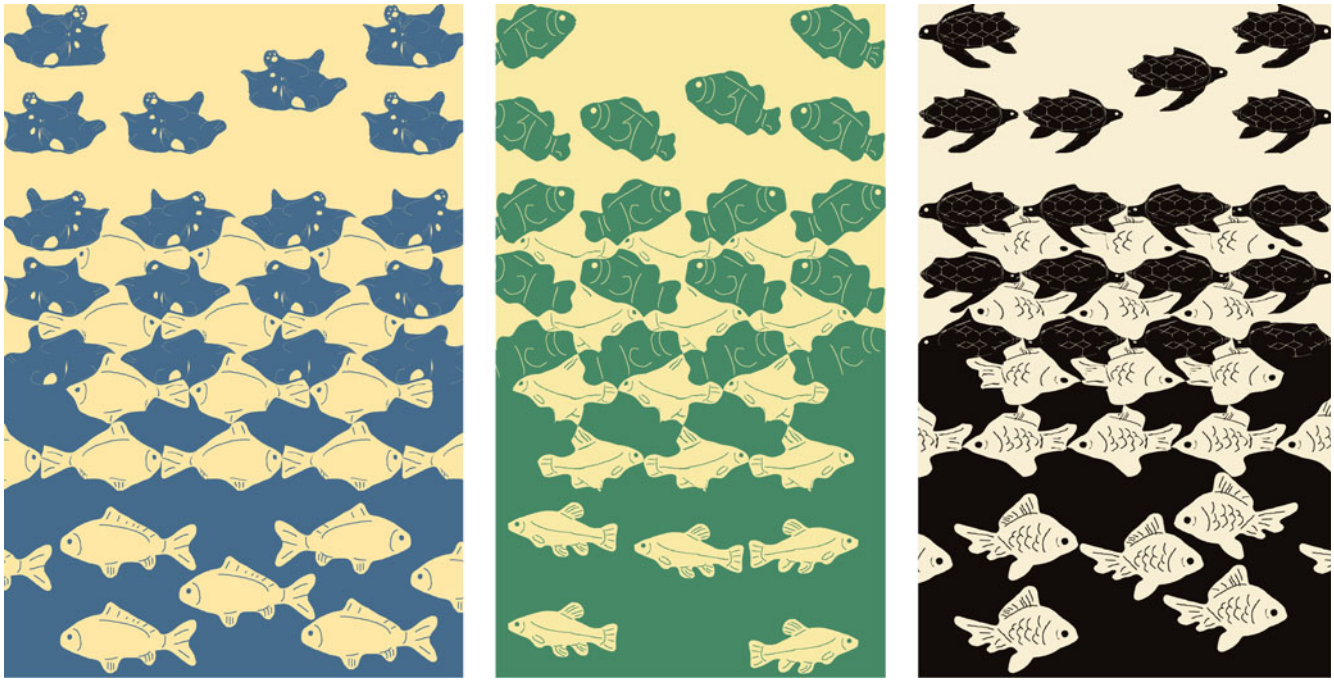

Fig. 12. Results of less regular transmutations.

matched to the subsequent tile. Fourth, the tiling crossfade in Escher's artworks is implemented by assigning a significance value to each feature line inside the tiles. Several examples are shown in Fig. 10. The features lines of tiles are gradually removed to smooth the tile transition. Fifth, the sky-and-water deformation used in the Escher's *Sky-and-Water* works can be generated by integrating the deformations of interpolation, abutment, and crossfade. An example is shown in Fig. 11 (top-right). A fish tile progressively disappears into the background while the background gradually reveals the shape of a bird in the dual space. In addition, the proposed methods also can generate less regular tilings, as shown in Fig. 12. Our system also allows users to produce single-tile tessellation, as shown in Fig. 13, in addition to Escher transmutation generation. However, the single-tile tessellation is not a pure monohedral tiling since the shapes of the source and target tiles are deformed by warping. The proposed system with these tilings and deformations allows artists and even general users to efficiently create various Escher-like transmutations, which can be used in advertisement and commercial design.

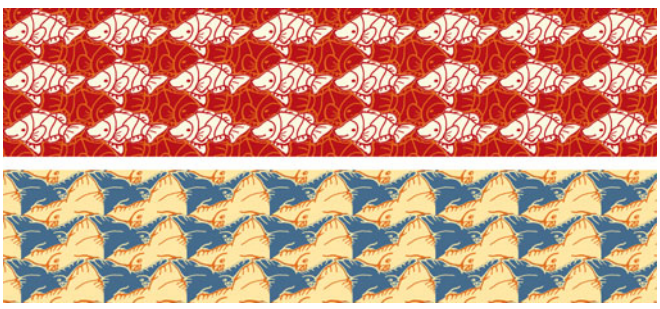

Fig. 13. The tessellation results generated using a single-tile as both the source and virtual tiles.

4.2 Evaluation of The Proposed Method

We implement and evaluate our system on a PC with 3.4 GHz quad-core CPU and 4 GB RAM. For a dataset containing 187 tiles, the average computation time for tile initiation, shape matching per tile, feature line simplification, and shape transmutation are 0.08, 0.41, 0.23, and 4.34 seconds, respectively. The computational bottleneck is the shape matching that requires searching for the best-matched tile in the database. This process can be significantly speeded-up by using multi-core CPU and GPU computation. For larger datasets, user-specified thematic constraints and a categorical database can be used to control the computational time needed to search for the optimal candidate tiles. For example, a large set of animal shapes can be categorized by classifiers such as family, genus, or species. Then, a user can specify a category for the matching animal so that only those types of shapes are checked.

To demonstrate the feasibility of the proposed methods, various tiling and transmutation results are generated. Several cases where the tiles have similar geometric shapes are demonstrated in Figs. 10, 11, and 12. In these cases, the first tile is user-selected and the other tiles are determined with the aid of the proposed tile retrieval method. Additionally, some specific cases where the tiles have clearly mismatched shapes are tested (Fig. 9). In these cases, the tiles are selected manually and the shape matching is performed to obtained an appropriate alignment of the tiles.

Compared with the related work [15], the proposed method not only focuses on shape matching, but also preserves the feature lines inside the tiles. Therefore, the deformed tiles generated by our method have better recognizable results than those of [15], as shown in Fig. 11. Compared with the related works [12] and [14] that focus on the escherization problem to generate isohedral tiling patterns, our study addresses on the generation of Escher-like transmutations with dual figure-ground perception. With the

TABLE 1
User Study Results

	Aesthetics	Smoothness	Duality	Average
Sugihara [15]	3.36	3.21	3.25	3.27
Ours	3.77	3.55	3.71	3.68
t-test	$t(558) = 5.39, p < .001$	$t(558) = 3.89, p < .001$	$t(558) = 6.05, p < .001$	$t(1678) = 8.75, p < .001$

The scores range from 1.0 (the lowest score) to 5.0 (the highest score).

deformations of crossfade, duality, growth, and interpolation, our system can generate various Escher-like transmutations, as shown in Figs. 10, 11, and 12.

User Study. To evaluate the proposed system, the generated results are compared with those in [15]. The comparisons are shown in Fig. 11. In addition, a user study involving 70 participants aged 20 years old to 52 years old is conducted. The 65 participants were college students, and the others were college professors and artists. The participants are shown several Escher-like transmutations generated by our method and those of [15], and the participants are asked to evaluate each of them, in terms of aesthetic quality, smoothness of shape transition, and dual perception effect. The survey results in Table 1 indicate that the participants prefer our results which have better scores of aesthetics, smoothness, and duality. To measure the statistical significance of the user study, a two-sample t-test is utilized to compare the mean difference between the tilings generated by [15] and the proposed method. The test indicates that the mean difference of properties among those Escher-like transmutations is significant as $p < .001$. A possible reason is the progressive texture representation in our results can enhance figure-ground dual perception and enrich tile presentation. The visual comparisons and the user study demonstrate that our results are better than those of [15] in terms of duality effect and figure-ground representation.

Limitation. At present, our system cannot handle tiles with extremely mismatched shapes. The mismatched shapes lead to a significant deformation in warping, which may make the deformed tiles unrecognizable and may decrease the ambiguous figure-ground effect even though the interior feature lines are well preserved. For instance, in Fig. 14, the shapes of the input fish tiles are mismatched. The deformed tiles in the red quadrangle are almost unrecognizable. Fortunately, this case is rare when a database containing a large variety of tiles is available. A pair of well-matched tiles can be extracted using the proposed shape matching and retrieval method.

Fig. 14. Escher-like transmutation of mismatched tiles. The recognizability of the deformed tiles is significantly decreased because of the tile mismatch.

5 Conclusions and Future Work

Inspired by Escher's transmutation artworks, this study utilized several graphic techniques, including shape matching, warping, and simplification, to generate Escher-like transmutations. The deformation types, crossfade, abutment, growth, sky-and-water, and interpolation, which are commonly used in Escher's artworks are implemented and provided in our system. Therefore, various Escher-like transmutations can be generated. The visual comparisons and conducted user study showed that our results are better than those of [15], in terms of aesthetics, smoothness, and figure-ground dual perception. Therefore, we conclude that the proposed method can generate Escher-like artworks through several engineering procedures without the help of artistic design. Moreover, our system can be a tool for both artistic and inartistic users to efficiently create an elegant Escher-like transmutation. According to the taxonomy presented by Kaplan [2], the proposed system is capable of generating five of the six varieties of transition devices used in Escher's artwork. In the future, we plan to complete the taxonomy by adding the transition device, "*realization*" to the system. Unlike the other five varieties, "*realization*" dissolves a single shape into a landscape or other concrete scene. Incorporating "*realization*" into our proposed system would allow users to blend all six varieties of transition devices the way Escher did in his masterpiece *Metamorphosis II*. Furthermore, determining appropriate significance values for a shape's boundary points could be useful in alleviating the unfavorable distortion resulting from warping poorly matched shapes. Considering the contour saliency could also be useful in enhancing the dual figure-ground perception of the generated transmutation.

Acknowledgments

The authors would like to thank the anonymous reviewers for their constructive comments to improve the manuscript. This research was supported in part by the Ministry of Science and Technology (contracts MOST-106-2221-E-006-233-MY2 and MOST 105-2634-E-019-001), Taiwan.

References

[1] F. H. Bool, J. R. Kist, F. Wierda, and J. L. Locher, *M.C. Escher: His Life and Complete Graphic Work*, New York, NY, USA: H. N. Abrams, Abradale Press, 1992.
[2] C. S. Kaplan, "Metamorphosis in Escher's art," in *Proc. Math. Connections Art Music Sci.*, 2008, pp. 39–46.
[3] J. Kim and F. Pellacini, "Jigsaw image mosaics," *ACM Trans. Graph.*, vol. 21, no. 3, pp. 657–664, 2002.
[4] X. Xu, L. Zhang, and T.-T. Wong, "Structure-based ASCII art," *ACM Trans. Graph.*, vol. 29, no. 4, pp. 52:1–52:10, 2010.
[5] N. J. Mitra and M. Pauly, "Shadow art," *ACM Trans. Graph.*, vol. 28, no. 5, pp. 156:1–156:7, 2009.

[6] M.-T. Chi, T.-Y. Lee, Y. Qu, and T.-T. Wong, "Self-animating images: Illusory motion using repeated asymmetric patterns," *ACM Trans. Graph.*, vol. 27, no. 3, pp. 62:1–62:8, 2008.
[7] R. Maharik, M. Bessmeltsev, A. Sheffer, A. Shamir, and N. Carr, "Digital micrography," *ACM Trans. Graph.*, vol. 30, no. 4, pp. 100:1–100:12, 2011.
[8] H.-K. Chu, W.-H. Hsu, N. J. Mitra, D. Cohen-Or , T.-T. Wong, and T.-Y. Lee, "Camouflage images," *ACM Trans. Graph.*, vol. 29, no. 4, pp. 51:1–51:8, 2010.
[9] C. D. Becker, "Creating repeating hyperbolic patterns based on regular tessellations," *Thesis*, Faculty Graduate School, Univ. of Minnesota Duluth, Duluth, MN, USA, 2012.
[10] B. de Smit and H. W. Lenstra Jr, "Artful mathematics: The heritage of M.C. Escher," *Notices Amer. Math. Soc.*, vol. 50, no. 4, pp. 446–451, 2003.
[11] J. Yen and C. Séquin, "Escher sphere construction kit," in *Proc. Symp. Interactive 3D Graph.*, 2001, pp. 95–98.
[12] C. S. Kaplan and D. H. Salesin, "Escherization," in *Proc. 27th Annu. Conf. Comput. Graph. Interactive Tech.*, 2000, pp. 499–510.
[13] H. Koizumi and K. Sugihara, "Maximum eigenvalue problem for escherization," *Graphs Combinatorics*, vol. 27, no. 3, pp. 431–439, 2011.
[14] C. S. Kaplan and D. H. Salesin, "Dihedral escherization," in *Proc. Graph. Interface*, 2004, pp. 255–262.
[15] K. Sugihara, "Computer-aided generation of Escher-like sky and water tiling patterns," *J. Math. Arts*, vol. 3, no. 4, pp. 195–207, 2009.
[16] M. A. Peterson and E. Salvagio, "Inhibitory competition in figure-ground perception: Context and convexity," *J. Vis.*, vol. 8, no. 4, pp. 1–13, 2008.
[17] S. E. Palmer and J. L. Brooks, "Edge-region grouping in figure-ground organization and depth perception," *J. Exp. Psychology Human Perception Perform.*, vol. 34, no. 6, pp. 1353–1371, 2008.
[18] M. Bertamini and R. Lawson, "Rapid figure-ground responses to stereograms reveal an advantage for a convex foreground," *Perception*, vol. 37, no. 4, pp. 483–494, 2008.
[19] M. A. Peterson, *Low-Level and High-Level Contributions to Figure-Ground Organization*. In J. Wagemans (Ed.), Oxford, U.K.: Oxford Univ. Press, 2013.
[20] D. Schattschneider, "Lessons in duality and symmetry from M.C. Escher," in *Proc. Math. Connections Art Music Sci.*, 2008, pp. 1–8.
[21] M. Cui, J. Femiani, J. Hu, P. Wonka, and A. Razdan, "Curve matching for open 2D curves," *Pattern Recog. Lett.*, vol. 30, no. 1, pp. 1–10, 2009.
[22] J. R. Shewchuk, "Triangle: Engineering a 2D quality mesh generator and Delaunay triangulator," in *Proc. Sel. Papers Workshop Appl. Comput. Geom. Towards Geom. Eng.*, 1996, pp. 203–222.
[23] A. Altman and J. Gondzio, "Regularized symmetric indefinite systems in interior-point methods for linear and quadratic optimization," *Optimization Methods Softw.*, vol. 11, pp. 275–302, 1999.

Shih-Syun Lin received the MS degree from the Graduate Institute of Educational Measurement and Statistics, National Taichung University, Taiwan, in 2010 and the PhD degree in computer science and information engineering from National Cheng-Kung University, Taiwan, in 2015. He was as a postdoctoral fellow in the Computer Graphics Group of Visual System Laboratory (CGVSL), National Cheng-Kung University, Taiwan, from 2015 to 2016. He currently is an assistant professor in the Department of Computer Science and Engineering, National Taiwan Ocean University, Taiwan. He leads the Intelligent Graphics Laboratory, National Taiwan Ocean University (http://igl.cse.ntou.edu.tw). His research interests include computer graphics, information visualization, and pattern recognition. He is a member of the IEEE and the ACM.

Charles C. Morace received the BS degree in computer science and mathematics from the University of Rhode Island, in 2012. He began graduate study in the Department of Computer Science and Information Engineering, National Cheng-Kung University, Tainan, Taiwan, ROC, in 2014, where he is currently working toward the PhD degree in the Computer Graphics Group of the Visual System Laboratory. His research interests include computer graphics, visualization, and digital map generation.

Chao-Hung Lin received the MS and PhD degrees in computer science and information engineering from National Cheng-Kung University, Taiwan, in 1998 and 2004, respectively. Since 2006, he has been a member of the faculty of the Department of Geomatics, National Cheng-Kung University. He currently is a professor. He leads the Digital Geometry Processing Laboratory (http://dgl.geomatics.ncku.edu.tw) and co-leads the Computer Graphics Laboratory, National Cheng-Kung University (http://graphics.csie.ncku.edu.tw). His current research interests include remote sensing, point cloud processing, digital map generation, information visualization, and computer graphics. He served as an editorial board member of the *International Journal of Computer Science and Artificial Intelligence*. He is a member of the IEEE.

Li-Fong Hsu received the BS degree from the Department of Computer Science and Information Engineering, Cheng-Kung University, Taiwan, in 2013 and the MS degree from the Department of Computer Science and Information Engineering, National Cheng-Kung University, Taiwan, in 2015. Now, he is working in Synology Inc. His research interest is computer graphics.

Tong-Yee Lee received the PhD degree in computer engineering from Washington State University, Pullman, in May 1995. He is currently a chair professor in the Department of Computer Science and Information Engineering, National Cheng-Kung University, Tainan, Taiwan, ROC. He leads the Computer Graphics Group, Visual System Laboratory, National Cheng-Kung University (http://graphics.csie.ncku.edu.tw/). His current research interests include computer graphics, non-photorealistic rendering, medical visualization, virtual reality, and media resizing. He is a senior member of the IEEE and the member of the ACM.